AD-A105 532 TEXAS INSTRUMENTS INC DALLAS CENTRAL RESEARCH LABS F/G 9/1
DEVELOPMENT OF FABRICATION TECHNOLOGY FOR THE PERMEABLE BASE TR--ETC(U)
SEP 81 W R FRENSLEY, G H WESTPHAL N00014-80-C-0246

UNCLASSIFIED NL

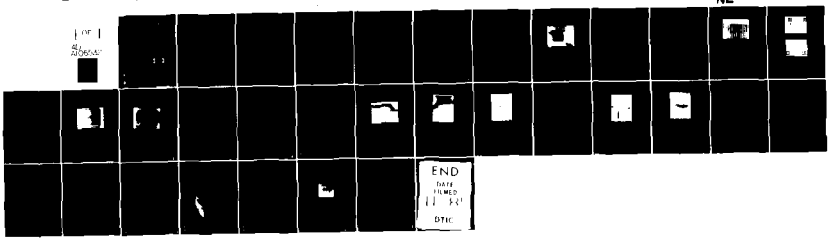

(15) LEVEL II

DEVELOPMENT OF FABRICATION TECHNOLOGY FOR THE PERMEABLE BASE TRANSISTOR

Texas Instruments Incorporated
Central Reserach Laboratories
13500 North Central Expressway
Dallas, Texas 75265

September 1981

Technical Report for Period 1 February 1980 - 31 March 1981

Contract No. N00014-80-C-0246

Contract Authority NR 251-042

Prepared for

Office of Naval Research
800 North Quincy Street
Arlington, Virginia 22217

Unclassified

SECURITY CLASSIFICATION OF THIS PAGE (When Data Entered)

REPORT DOCUMENTATION PAGE

READ INSTRUCTIONS BEFORE COMPLETING FORM

1 REPORT NUMBER

2. GOVT ACCESSION NO. AD-A10553

3. RECIPIENT'S CATALOG NUMBER 2 (9)

4 TITLE (and Subtitle)

(6) Development of Fabrication Technology for the Permeable Base Transistor,

5. TYPE OF REPORT & PERIOD COVERED Annual Report, 1 Feb 1980 – 31 Mar 1981

6. PERFORMING ORG. REPORT NUMBER

7 AUTHOR(s)

(10) W. R. Frensley

G. H. Westphal

8. CONTRACT OR GRANT NUMBER(s)

(15) N00014-80-C-0246 mod

9 PERFORMING ORGANIZATION NAME AND ADDRESS

Texas Instruments Incorporated
Central Research Laboratories
Dallas, Texas 75265

10. PROGRAM ELEMENT, PROJECT, TASK AREA & WORK UNIT NUMBERS

11 CONTROLLING OFFICE NAME AND ADDRESS

(11)

12. REPORT DATE 1 September 1981

13. NUMBER OF PAGES

14 MONITORING AGENCY NAME & ADDRESS (if different from Controlling Office)

Physical Sciences Division
Office of Naval Research
800 North Quincy Street
Arlington, Virginia 22217

(12)

15. SECURITY CLASS. (of this report) Unclassified

15a. DECLASSIFICATION DOWNGRADING SCHEDULE

16 DISTRIBUTION STATEMENT (of this Report)

DISTRIBUTION STATEMENT A
Approved for public release;
Distribution Unlimited

17 DISTRIBUTION STATEMENT (of the abstract entered in Block 20, if different from Report)

Distribution limited to U.S. Government Agencies only. Other requests for this document must be referred to DARPA/TIO.

18 SUPPLEMENTARY NOTES

19. KEY WORDS (Continue on reverse side if necessary and identify by block number)

Permeable base transistor
Epitaxial growth
Gallium arsenide
Electron beam lithography
arsenic trichloride

20 ABSTRACT (Continue on reverse side if necessary and identify by block number)

Efforts during the first year of this contract have concentrated on the development of the key processes required for fabrication of the permeable base transistor: sub-micrometer lithography and epitaxial overgrowth. Electron beam lithography was used, with a dry-process resist and ion milling, to produce 0.25 micrometer lines. The $AsCl_3$ epitaxial process was used to embed metal structures

DD FORM 1 JAN 73 1473 EDITION OF 1 NOV 65 IS OBSOLETE

Unclassified 403833

SECURITY CLASSIFICATION OF THIS PAGE (When Data Entered)

20

in a single crystal of GaAs. High-resolution electron microscopy revealed that the epitaxial overgrowth was imperfect, leaving voids in the single crystal which are often too small to be resolved using conventional electrom microscopy.

TABLE OF CONTENTS

LIST OF ILLUSTRATIONS

LIST OF ILLUSTRATIONS

(Continued)

SECTION I INTRODUCTION

This report describes work performed at Texas Instruments to develop permeable base transistor (PBT) devices[1] under ONR Contract N00014-80-C-0246. The period covered is from 1 February 1980 to 31 March 1981.

1 C. O. Bozler and G. D. Alley, "Fabrication and Numerical Simulation of the Permeable Base Transister," IEEE Transactions on Electron Devices, ED-27, 1128 (1980).

SECTION II
PROCESS DEVELOPMENT

A. Submicrometer Lithography

The PBT requires the definition of lines and spaces with dimensions well under one micrometer if a structure with the desired control properties is to result. This implies that optical lithography will not be adequate, and therefore techniques such as electron beam or x-ray lithography must be used. Moreover, the process by which a pattern is transferred to the final device structure has a profound impact on the achievable resolution of any technique. The PBT requires only a thin metal structure with submicrometer resolution and with no critical alignment. Thus it is possible to contemplate the fabrication of this device with presently available technology.

Initial efforts to develop an ultrafine lithography technology for the PBI concentrated on a lift-off process with e-beam definition and positive resist. This approach typically resulted in the fabrication of a microscopically corrugated metal foil, rather than a series of lines and spaces (Figure 1). The difficulties with this approach may be attributed to the properties of the lift-off process. Lift-off requires a very sharply defined resist pattern in order to cleanly separate the lifted from the unlifted metal. As the dimensions are reduced, however, the sharpness of the pattern decreases. With electron beam lithography this is caused by of the finite width of the beam and exposure of the resist by electrons backscattered from the substrate. The result is that the remaining "unexposed" resist is thin and of a rounded cross section, as may be inferred from Figure 1.

Another aspect of the PBT process that makes it difficult to use lift-off is the need for very refractory metals. In particular, tungsten and some of its alloys are the only materials that have demonstrated the ability to survive the epitaxial process. The problem concerns the temperatures to which the resist is exposed during the deposition process. Tungsten has the highest

Figure 1 The Results of an Unsuccessful Lift-Off Process with E-Beam Defined Lines on 0.25 μm Centers. The pattern should have been a series of lines connected by the pad area at the right. Part of the metal has torn and lifted off the slice, making it obvious that the fabricated structure is really a corrugated metal foil.

heats of fusion and vaporization as well as the highest melting temperature of any of the elements. Thus, during evaporation the slice receives a great deal of thermal energy by direct radiation (the source is hotter than an incandescent filament and of appreciable area) and is also heated by the heat released from the condensation of the tungsten. This does not have a beneficial effect on the organic polymers of the photoresist. In early tungsten evaporation experiments it was found that the resist would usually flow, resulting in degraded patterns and torn metal edges.

In view of the above difficulties, Texas Instruments decided to investigate alternative lithographic processes, particularly those involving selective removal rather than selective deposition. Tungsten can be removed in several ways, including wet etching, plasma etching, and ion milling. Wet etching in H_2O_2 proved to be unsatisfactory. The unetched area of the tungsten was frequently observed to peel off the slice after wet etching. There is also a question of the effectiveness of wet etching at very small geometries because of the problem of wetting very small cavities. (Note that there is a significant difference between the processes of resist development and a subsequent etching step. In the first case, an initially planar surface is easily wetted and remains wetted as the surface relief develops. In the second case, the liquid must enter the existing cavities. The reliability with which this is done depends upon the properties of the surface to be wetted, but it certainly becomes less reliable as the size of the structure decreases.)

Plasma etching also proved unsuitable. Tungsten should etch in a CF_4 plasma, but experimental efforts to etch tungsten layers deposited on glass slides resulted in nonuniform and incomplete removal of the tungsten. It is not known whether this is caused by contaminants in the tungsten or by plasma etching conditions.

Ion milling produced the best results in fabricating submicrometer tungsten lines. Two different masking techniques were employed with ion milling. The first was a process used to make optical-resolution lines for development of the epitaxy process. Positive photoresist was used on silicon nitride. The lines were defined in the photoresist and subsequently transferred to the silicon nitride by plasma etching. The combination of resist and nitride was then used as the milling mask. The resulting patterns are shown in Figure 2, and the optical mask used to form them is shown in Figure 3. The second masking process employed the dry-process negative resist described below. This was developed for electron beam definitions, but it also proved useful for optical exposure.

The use of ion milling to define the metal raises unresolved questions about damage to the underlying GaAs. Ion milling certainly removed GaAs, and presumably creates damage in the process. However, the removal of some GaAs will be beneficial in that it will also remove any surface contamination. Also, the overgrown structure can be thermally annealed to remove residual damage, and the epitaxy process itself should provide some annealing effect. It should be noted that TI has obtained epitaxially overgrown layers of apparently good crystallographic quality on ion-milled surfaces.

A major part of the process development effort has been directed toward the evaluation and development of a dry-process resist technology. TI has used Plasma-Rist (manufactured by Hercules Incorporated, Wilmington, Delaware). This is a negative resist that is sensitive to ultraviolet, electron beam, and x-ray exposure. It is spun onto the slice in the conventional manner, and then subjected to a soft bake to remove the solvent. After exposure the resist is baked at a higher temperature. After this bake, the exposed pattern is apparent in the surface relief of the resist, and the layer is no longer sensitive to exposure. The final development of the resist requires ashing in an oxygen plasma, where the unexposed portions are

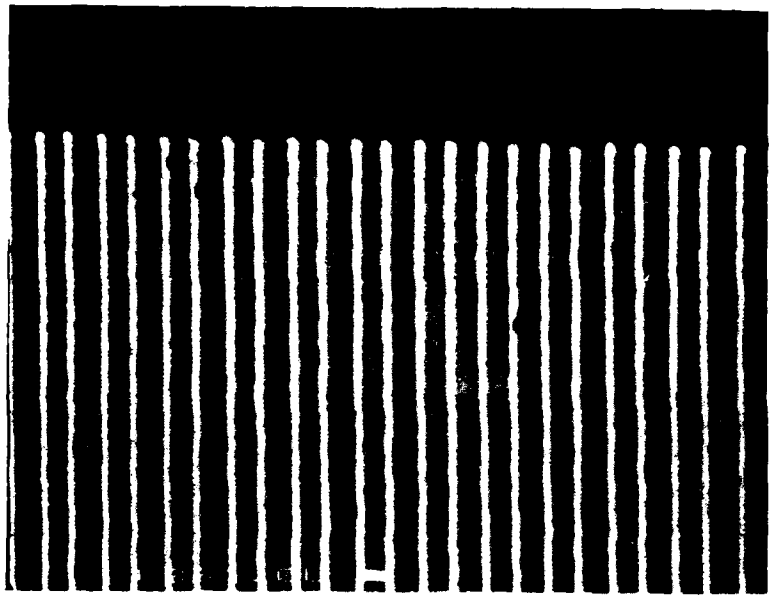

Figure 2 SEM Photo of a Tungsten Grid Pattern on GaAs Defined by Optical Lithography and Fabricated by Ion Milling. The total period (pitch) is 1.0 μm, as indicated by the scale marker, and the linewidth is approximately 0.25 μm.

(a)

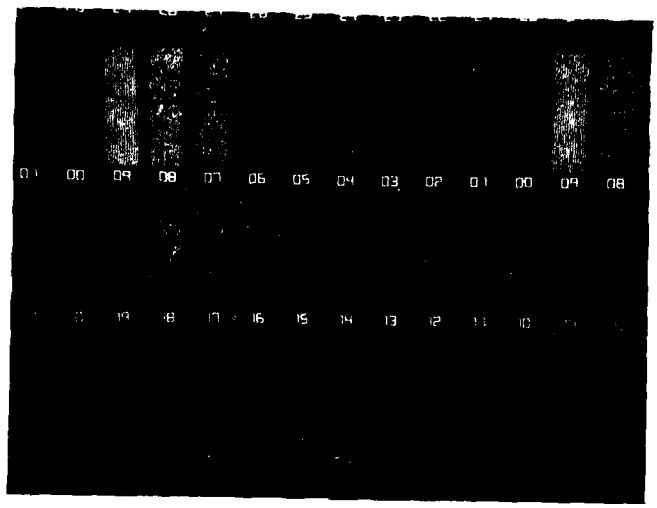

(b)

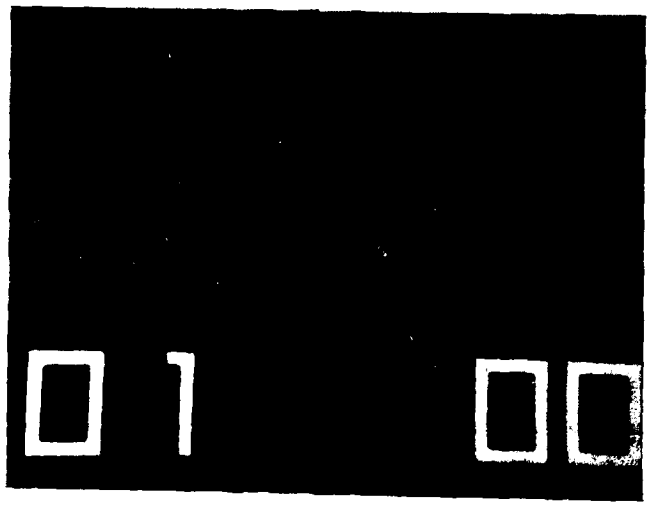

Figure 3 (a) E-Beam Fabricated Optical Resolution Series Mask.
(b) Close-up View of the Finest-Resolution Patterns. Pattern 01 consists of 0.5 μm lines on 1.3 μm pitch, while pattern 0.0 contains 0.4 μm lines on 1.0 μm pitch.

preferentially removed. Figure 4 shows a pattern of tungsten lines of 0.25 μm width on 0.5 μm centers, defined using e-beam exposure of Plasma-Rist and ion milling.

A period of 0.5 μm is the best resolution Texas Instruments has achieved with good definition. However, it is difficult to exploit such resolution in the device fabrication process. To assure that the resist is properly developed, the pattern must be able to be examined optically. (The SEM has trouble imaging uncoated resist.) We have therefore chosen to limit the active device patterns to periods of 0.8 and 1.0 μm, corresponding to nominal linewidths of 0.4 and 0.5 μm. Figure 5 shows part of an actual device pattern defined in Plasma-Rist.

The problem of providing alignment masks for the electron beam machine proved to be unexpectedly difficult. While the PBT required no critical submicrometer alignment, the e-beam fields should be stepped with sufficient accuracy to permit good alignment to subsequent optical levels. E-beam 1 is not equipped with an interferometer-controlled stage, and "open loop" stepping will accumulate several micrometers of error over a few hundred millimeters. Therefore, it is necessary to have some alignment marks on the slice to which each field may be aligned. The constraints imposed by the epi overgrowth process make the problem difficult, as marks must consist of either tungsten or GaAs. Various etched and lifted tungsten marks proved unsuitable. The solution proved to be etched alignment marks in the GaAs that were formed by an isotropic etching procedure using an HCl-based etchant.

Another aspect of the process that was investigated is the method of deposition of the metal. The sheet resistance of evaporated tungsten was compared to that of sputtered titanium-tungsten alloy. (This alloy is widely used in semiconductor processes because its metallurgical properties are superior to those of pure tungsten.) The evaporated tungsten had a sheet

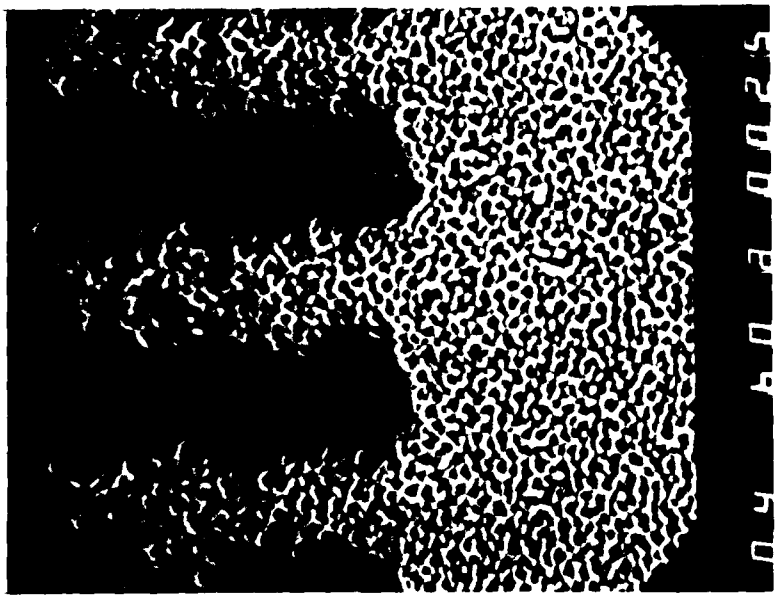

Figure 4 Tungsten Lines of 0.25 μm Width and 0.5 μm Period Defined by E-Beam Lithography with Dry-Process Resist and Ion Milling. This micrograph was taken on a scanning transmission electron microscope (STEM), in secondary electron mode, at a magnification of 60,000. The rather pronounced texture of the GaAs surface is of concern, but it may be caused by the processes used to prepare this sample for SEM examination.

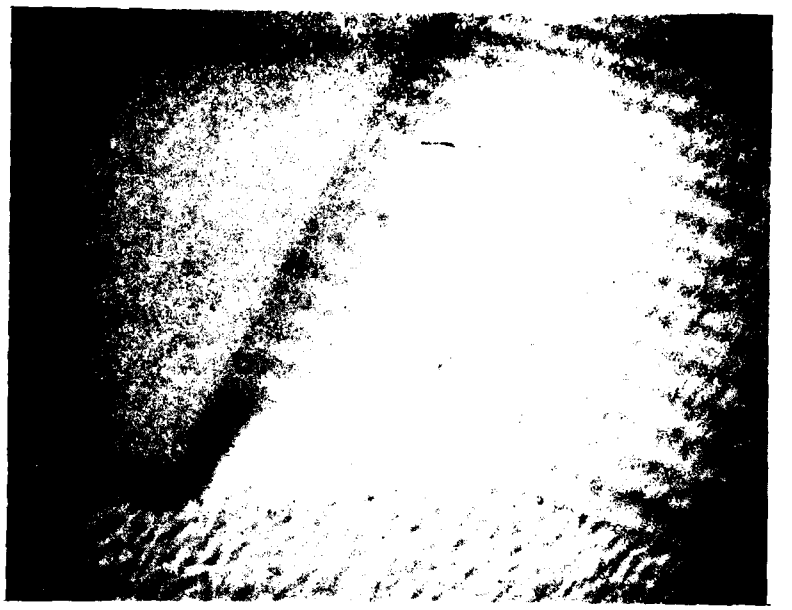

Figure 5 A Device Pattern Defined in Dry-Process Negative Resist. The lines are defined on a 0.8 μm period.

resistance of 80 Ω/square for a nominally 300 Å film. The sputterred Ti/W film had a sheet resistance of 10 Ω/square, but the thickness of this film was not precisely known, as there is no thickness monitor in the sputtering system. The optical densities of the films (they were deposited on glass slides) indicated that the Ti/W film was thicker, but certainly not thick enough to explain the factor of eight difference in sheet resistance. The bulk resistivity would indicate a sheet resistance on the order of 2 Ω/square. Thus it appears that the evaporated films are contaminated, presumably with oxygen.

A slice coated with Ti/W was subjected to the epitaxial process and the film survived intact. However, when an attempt was made to overgrow a patterned Ti/W layer the overgrowth was successful, but upon clearing the slice no evidence of the Ti/W was found. Further work on Ti/W has been deferred until the void problem discussed in the next section is solved.

SECTION III
MATERIALS DEVELOPMENT

The epitaxial growth to bury the gate electrodes is the key process permitting fabrication of the PBT. The first PBT devices[1] were made using the $AsCl_3$ vapor phase epitaxy (VPE) technique. This standard epitaxy technology in use at Texas Instruments, was used in the PBT development efforts. To date, overgrowth has been attempted on 43 slices. The resulting layers have shown a variety of surface morphologies and degrees of coverage. A major problem has been identified: there is a tendency for voids to form above the tungsten fingers. Those voids are often sufficiently small that they are not detectable by examination in a scanning electron microscope (SEM) of standard resolution.

The conditions used for the overgrowth experiments were similar to those typically used for $AsCl_3$-based VPE. The growth was performed in a small-bore (45 mm), two-bubbler reactor. A liquid gallium source was used at a temperature of 821°C. The deposition occured with the slice at 725°C. The slice was placed on a carrier slice of Cr-doped GaAs which was used to assure that the exposed area of GaAs was constant from run to run. The growth was carried out at a flow of 100 standard cubic centimeters per minute (SCCM) through the main bubbler, 30 SCCM through the bypass bubbler, and 50 SCCM through the doping source. Before growth, the slice was typically vapor etched by increasing the flow through the bypass bubbler to 60 SCCM for twelve minutes. The typical growth time was 55 minutes.

The effect of crystallographic orientation on the overgrowth process was investigated. The orientations of a number of slices were determined by anisotropic chemical etching. The optically defined tungsten lines were oriented on the surface of the slice [which is a few degrees off the (001) plane] in one of three principle crystallographic directions: <110>, $<\bar{1}10>$ or

<100>. Sixteen of the epitaxial growth runs were devoted to this experiment. The best coverage and surface morphology occured when the lines were oriented in the <$\bar{1}$10> direction, that is then the growth proceeded in a <110> direction Thus the preferred orientation of the PBT lines is perpendicular to the favored gate direction for mesa-etched FETs.

The epitaxially overgrown structures were evaluated primarily by cleaving the slice and examining the cross section with a scanning electron microscope (SEM). Figure 6 shows such a cross section of the first slice where overgrowth was attempted. The bright "dashed line" appearing below the surface at the original surface (as shown by the growth edge at the right of the photo) is naturally interpreted as the buried tungsten grating. This is considered an indication of a successful overgrowth. Therefore, problems such as improving the surface morphology and determining the optimum crystallographic orientation were addressed next.

In characterizing submicrometer lithographic structures, the capabilities of the scanning transmission electron microscope (STEM) to observe backscattered or secondary electrons are superior to those of a standard SEM. The STEM has a finer beam and, in fact, has a resolution better than 15 Å. Examination of the cleaved cross sections of overgrown slices revealed that voids are commonly formed in the overgrown layer in the vicinity of the tungsten stripes. These voids are usually too small to be resolved with a standard SEM. Figure 7 shows a cross section of the same slice as shown in Figure 6. Voids of a few hundred angstroms thickness are observed above the tungsten metal. Figure 8 shows another slice that is fairly typical of the samples that have been observed. Several voids are seen and the edges of the voids show enhanced electron emission. This is an important effect because it makes the voids hard to observe with a lower-resolution instrument. It is easy to misinterpret a bright area as an embedded metal finger when the real

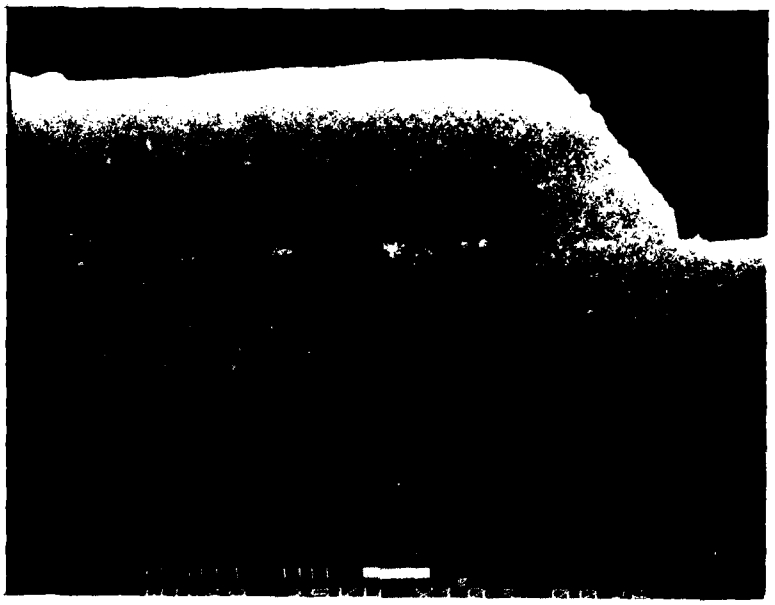

Figure 6 Cleaved Cross Section of Slice PBT-1. The micrograph was taken with a scanning electron microscope (SEM) of standard resolution. It shows an apparently successful coverage of the tungsten lines, apart from some areas on which no growth occured.

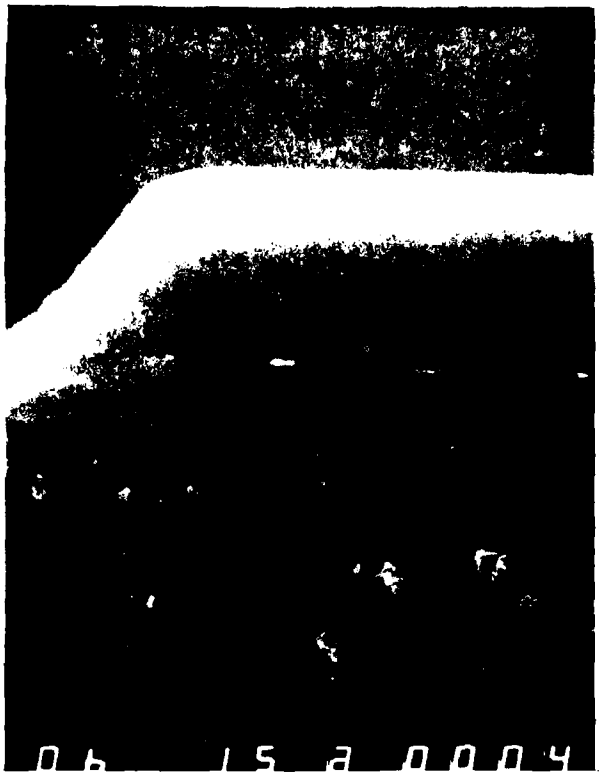

Figure 7 Micrograph of a Cleaved Cross Section of PBT-1 Taken with the STEM in SEM Mode. A very narrow void can be seen above the tungsten at far right.

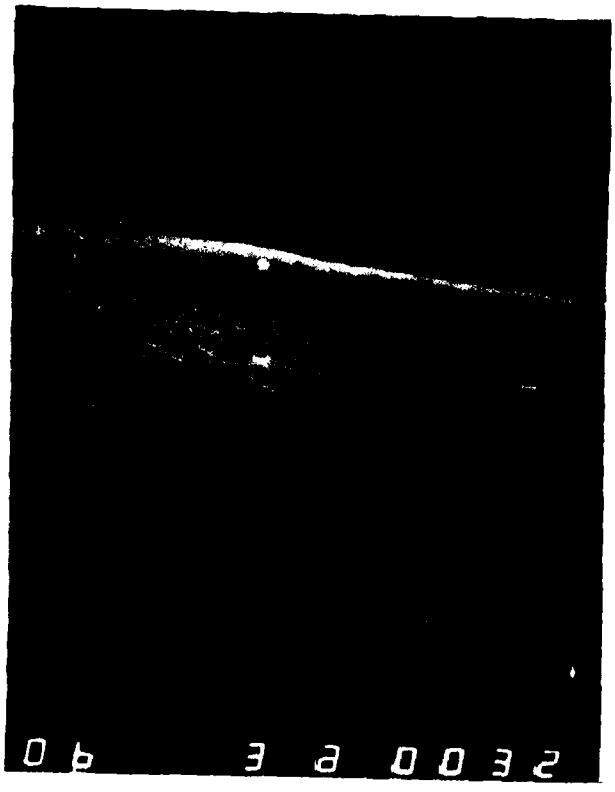

Figure 8 Typical Cross Section of a Slice Deemed "Good" from Standard SEM Examination. Three voids are apparent. The sample was tilted 30° away from the viewer to demonstrate the enhanced electron emission from the void edge that is easily misinterpreted as metal with a lower- resolution SEM. (Note the bright lower edge of the void.)

structure may be an empty void displaying enhanced edge emission. Figure 9 shows some voids which appear to be empty and some in which the tungsten is quite obvious.

None of the samples that we have examined in the STEM is entirely free from voids. However, there are examples of apparently good overgrowth, as shown in Figure 10. This picture, taken at a magnification of 150,000 shows a well enbedded tungsten finger with no obvious crystallographic imperfections in its vicinity. The nonuniform appearance of the tungsten is believed to be caused by irregular tearing of the tungsten during the cleaving process. The lenticular profile presumably reflects the profile of the original resist, with the outer edges of the resist being thinner and therefore more quickly removed during ion milling.

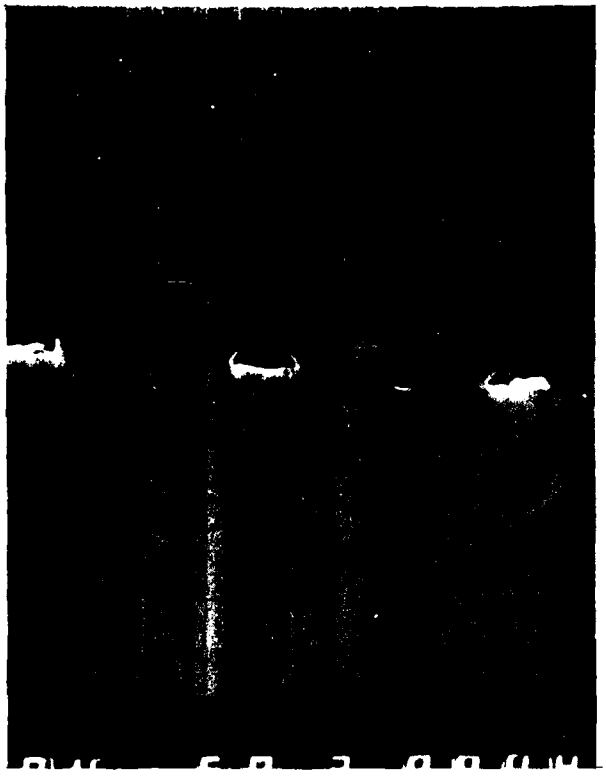

Figure 9 Voids in an Overgrown Slice. The lighter material remaining in the left- and right-most voids is tungsten. The magnification is 80,000.

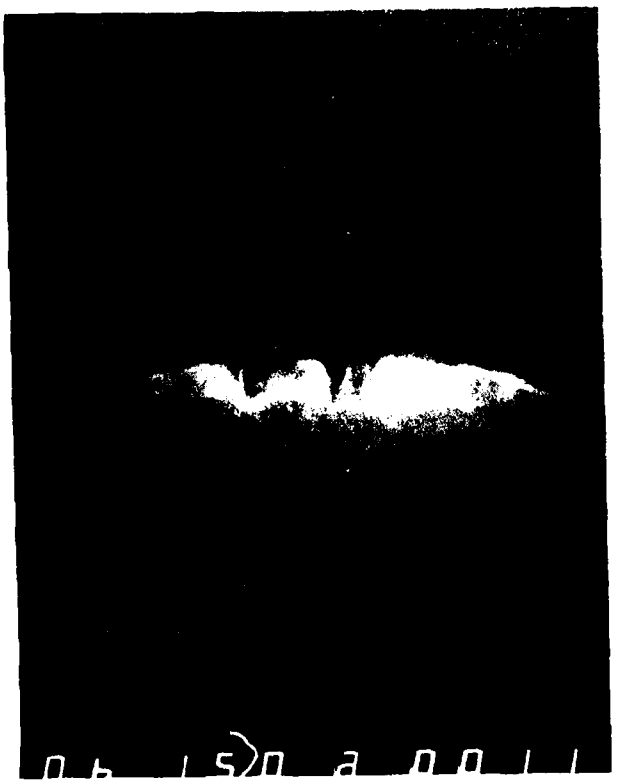

Figure 10 An Example of a Successful Covered Tungsten Stripe. The magnification is 150,000, and the thickness of the tungsten is 300 Å. The lenticular profile of the metal is believed to reflect the profile of the original resist.

SECTION IV
DEVICE DEVELOPMENT

A. Modeling

Because of the problems encountered in developing the PBT fabrication process, efforts to model the device have been somewhat de-emphasized. However, the study of the analytic model of sub-threshold mode of operation of the PBT has continued. This is the mode in which the current depends exponentially on the gate voltage. All field-effect devices exhibit this mode of operation at sufficiently low values of drain current, but because of the short effective gate length of the PBT, the subthreshold mode appears preeminently in the device characteristics. From the theoretical point of view, the subthreshold mode has the virtue of being analytically tractable. Because the current density is low, the contribution of the free carriers to the electrostatic potential can be ignored and thus Poisson's equation can be decoupled from the transport equations.

The geometry of the PBT model is shown in Figure 11. The width of each base finger is two times a, and the total period is two times b. The gate-to source depletion layer has a thickness d_1 and the gate-to-drain depletion layer has a thickness d_2. The electrostatic potential consists of two terms. One is the potential near a periodic array of charged conducting strips. This solution is readily found by complex variable techniques. The other term is simply the potential of a uniform charge distribution. The parameters of these terms are chosen so as to produce zero electric field and an equipotential along the depletion layer boundaries. (These conditions are satisfied only if d_1, $d_2 > b$.) The total electrostatic potential within the device is then given by

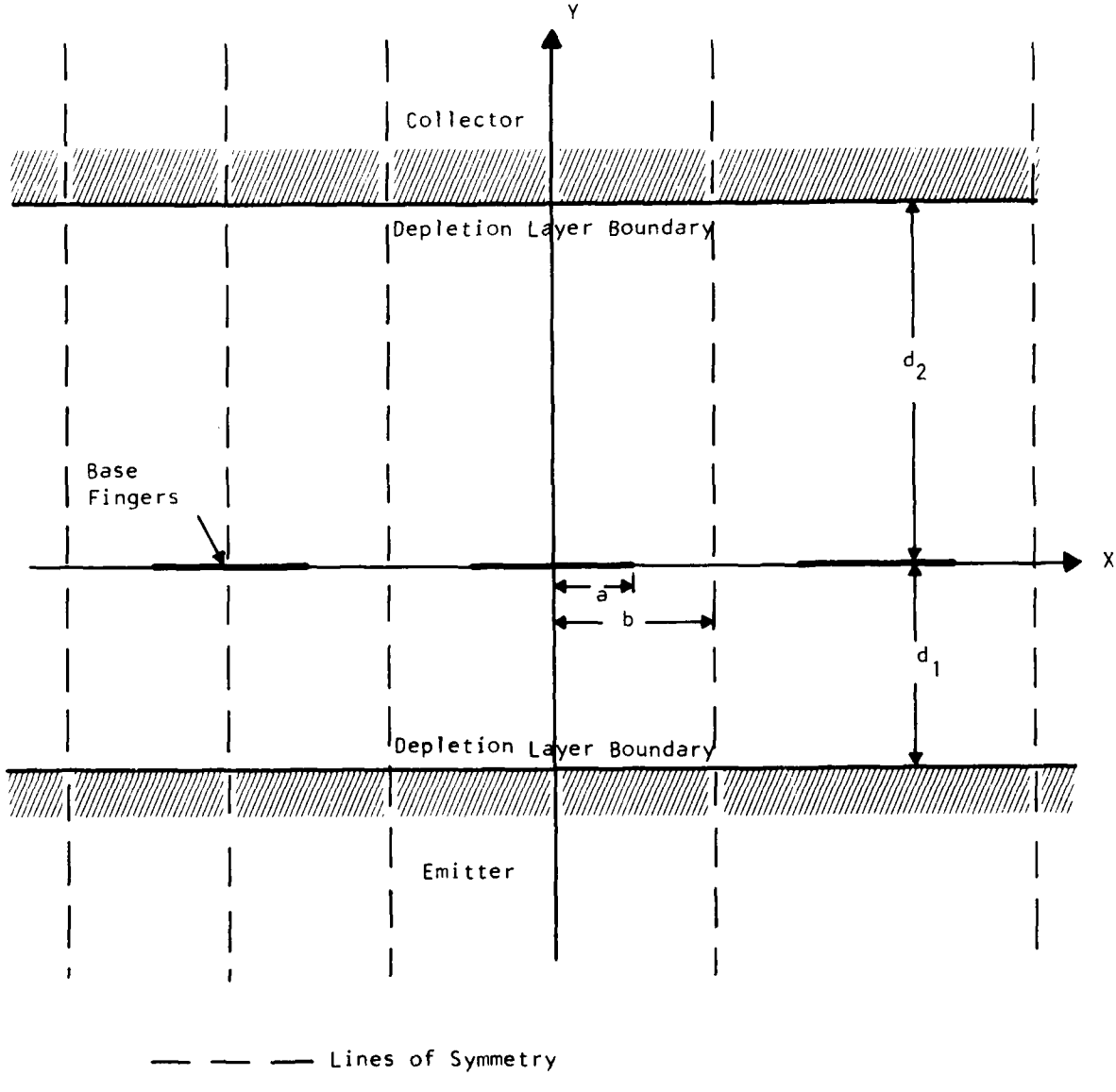

Figure 11 Geometry of the PBT Model

$$V(x,y) = V_G + \frac{qN\,(d_1 + d_2)b}{\pi\varepsilon} \quad \mathrm{Re}\left\{ \mathrm{COSH}^{-1}\left[\frac{\mathrm{Sin}\,(\pi z/2b)}{\mathrm{Sin}\,(\pi a/2b)} \right] \right\} - \frac{qN}{2\varepsilon}\left[y^2 - y\,(d_2 - d_1)\right] \qquad (1)$$

Here, N is the doping level, q is the elementary charge, ε is the dielectric constant, and $z = x + iy$. If we evaluate Equation (1) at the depletion layer boundaries, we can derive equations for d_1 and d_2 in terms of the terminal voltages V_S, V_G, and V_D:

$$d_1 = \sqrt{\frac{2\varepsilon}{qN}\,(V_S - V_G) + \frac{2b}{\pi}\,\ln\left[\mathrm{Sin}\,(\pi a/2b)\right]\,(d_1 + d_2)} \qquad (2a)$$

$$d_2 = \sqrt{\frac{2\varepsilon}{qN}\,(V_D - V_G) + \frac{2b}{\pi}\,\ln\left[\mathrm{Sin}\,(\pi a/2b)\right]\,(d_1 + d_2)} \quad . \qquad (2b)$$

These equations are readily solved by a simple iteration scheme.

Given the above electrostatic potential, we may now approach the transport problem. The current density $\vec{j}$ is given by the diffusion equation:

$$\vec{j} = q\mu n\,\vec{\mathcal{E}} - kT\mu\,\vec{\nabla} n, \qquad (3a)$$

or

$$\vec{j} = q\mu n\,\vec{\nabla}\,\Psi \quad , \qquad (3b)$$

if we introduce the quasi-Fermi level Ψ. Using the boundary conditions appropriate for the PBT, this equation can be integrated to give

$$\vec{j} = -q\mu N\,\frac{\exp\left[qV_C/kT\right] - \exp\left[qV_E/kT\right]}{\int_{-d_1}^{d_2} \exp\left[qV/kT\right]\,dy} \quad . \qquad (4)$$

To find the total current per unit width flowing through a channel we must integrate $\vec{j}$ over x, and to find the current per unit area we multiply by the channel width per unit area, which is simply 1/2b. Therefore, the current is

$$I = \frac{1}{2b}\int_0^{2b} \vec{j}\,dx \quad . \qquad (5)$$

Now the major contribution to the integrals in Equations (4) and (5) comes from the vicinity of the saddle point in V, which occurs near the gap between the metal fingers. The location of this saddle point is readily found by numerical calculation, and by calculating second derivatives at this point, the potential can be fitted to the form:

$$V = V_m + \frac{1}{2}\alpha^2 y2 - \frac{1}{2}\beta^2 x^2 \quad . \quad (6)$$

The integrals in Equations (4) and (5) are then evaluated, giving

$$I = \frac{\mu kTN}{2b}\frac{\alpha}{\beta}\left\{\exp\left[\frac{q}{kT}(V_m - V_S) - \exp\frac{q}{kT}(V_m - V_D)\right]\right\} \quad . \quad (7)$$

The results of this model are shown in Figure 12. Note that the characteristics are triode-like, which is to be expected for the low-current mode of operation. Unfortunately, these results do not indicate much about the ultimate performance of the device, because the best performance will be obtained at higher current levels, for which this model is not valid.

A clearer understanding of the subthreshold operation of the PBT can be gained by looking closely at the electrostatic potential. An isometric projection of a three-dimensional plot of the electrostatic potential is shown in Figure 13. The saddle points through which the electrons flow are apparent.

One aspect of PBT operation, which has not been generally recognized is that the "ideality factor" of the transfer characteristics will be rather large. If the drain current is expressed as

$$I \propto \exp(qV_G/nkT) \quad , \quad (8)$$

then n is the ideality factor and, by comparison of equations (7) and (8) is given by

$$n = \left(\frac{\partial V_m}{\partial V_G}\right)^{-1} \quad . \quad (9)$$

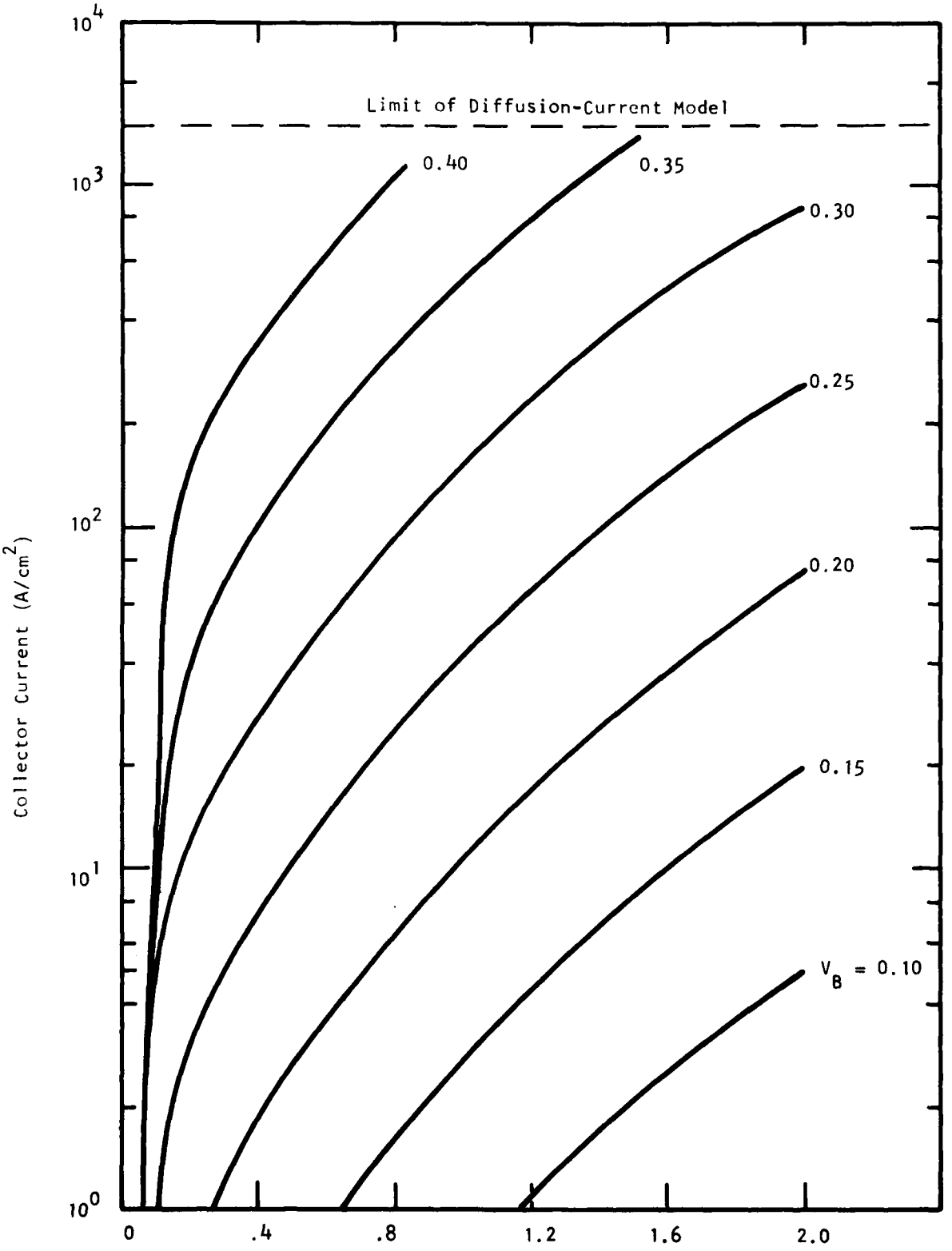

Figure 12 Device Characteristics Calculated from the Diffusion-Current Model of the PBT. The grid period is 3200 Å and the doping level is 1×10^{16} cm^{-3}.

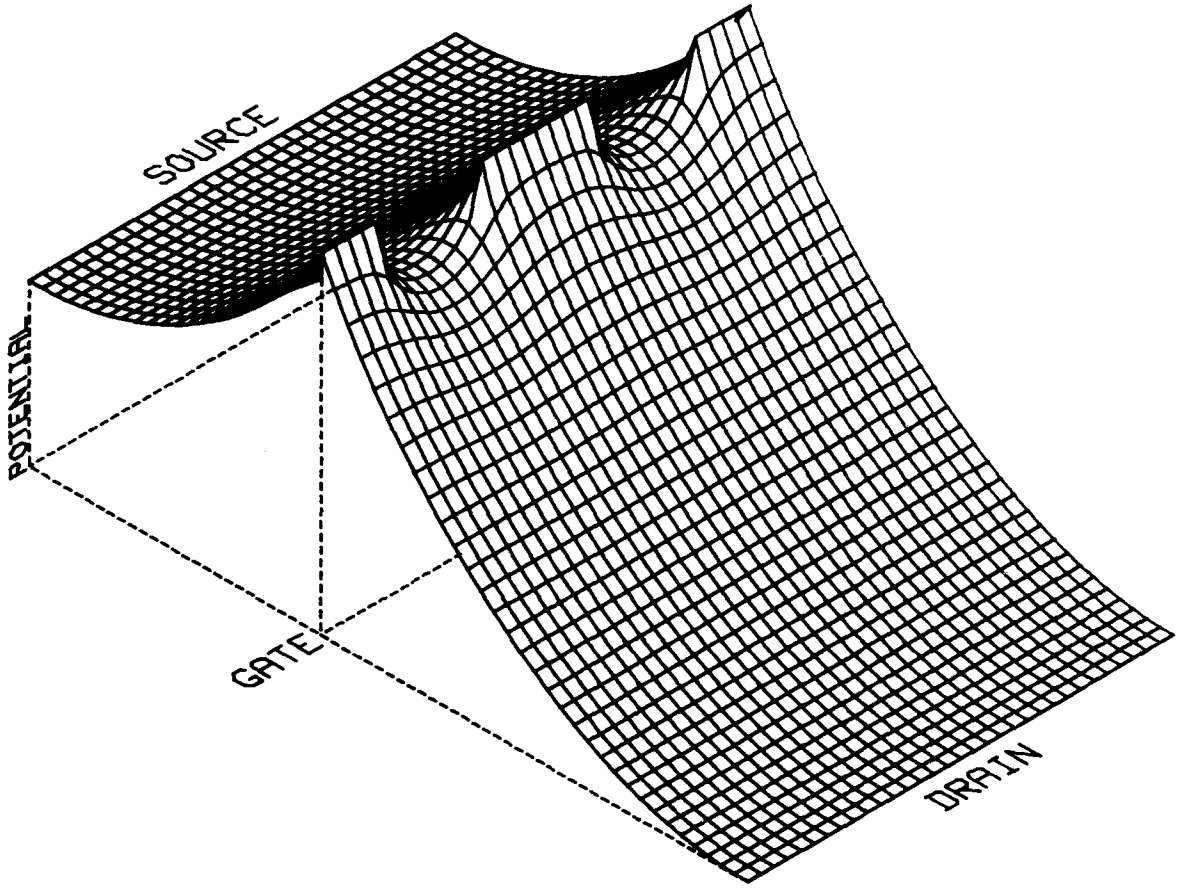

Figure 13 Plot of the Electrostatic Potential for a Model PBT

Because of the "averaging" properties of Poisson's equation, a change in the gate voltage will induce something less of a change in the saddle-point voltage V_m. Therefore,

$$\left.\frac{\partial V_m}{\partial V_G}\right|_{V_S,\, V_D} < 1 \quad .$$

Consequently n must be greater than 1. The exponential dependence postulated in (8) is not exact, and hence n will vary with bias voltage, but typically n will be greater than 2. (This effect can be intuitively understood by viewing Figure 4 and imagining that it represents the shape of a sheet of rubber. As the points of support at the gate are moved up and down, the height of the saddle point will follow this motion, but with a smaller magnitude.)

B. Device Design

A mask set for the fabrication of active PBT devices was designed and fabricated on e-beam VI. The e-beam defined tungsten level of this design is shown in Figure 14. (This level gives the most information about the device layout.) The design includes two devices of design similar to the Lincoln Laboratory design, with different line periods. It also includes two devices with larger active areas and two test structures of similar design, but which have two contact pads to facilitate measurement of the conductivity of the tungsten lines. Other test and alignment patterns are included on the mask.

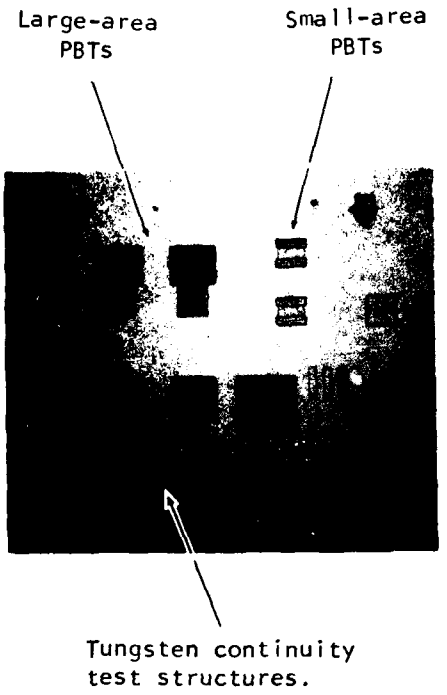

Figure 14 The E-Beam Defined Level of the PBT Mask Set

SECTION V
PLANS

The formation of voids during the epitaxial overgrowth process presents a major barrier to the development of a viable PBT process. Solution of this problem is likely to require some extremely detailed studies of the fundamental growth processes. While a slice containing active PBT devices will continue processing to completion, it is felt that producible high-performance devices are more likely to result from a process that does not require the epitaxial overgrowth. Accordingly, Texas Instruments is beginning to investigate devices which could be formed by etching high aspect-ratio grooves into GaAs and the processes by which such structures could be fabricated.

END

DATE
FILMED
11-81

DTIC